

RELATIONSHIP BETWEEN PARAMETERS OF THE FSP PROCESS AND TORQUE ACTING ON A TOOL

Marek S. Węglowski

Abstract

The effect of rotational and travelling speeds and down force on the torque in Friction Stir Processing (FSP) process is presented. The relationship between rotational speed and torque was modelled by an exponential function. The dependence of the travelling speed and down force affecting the torque was successfully approximated by linear functions. To find a dependence combining the spindle torque acting on the tool with the rotational speed, travelling speed and down force the artificial neural networks was applied. Studies have shown that the increase of rotational speed causes the decrease of torque while the increase in the travelling speed and down force causes the increase of the torque at the same time. Tests were conducted on casting aluminium alloy AlSi9Mg. Application of FSP process resulted in a decrease of the porosity in the modified material and refined microstructure.

Keywords: Friction Stir Processing, spindle torque, aluminium alloys

Analiza zależności parametrów procesu tarcowego modyfikowania warstwy wierzchniej i momentu obrotowego narzędzia

Streszczenie

W pracy przedstawiono wpływ prędkości obrotowej i przesuwu oraz siły docisku na moment obrotowy w procesie modyfikowania warstw wierzchnich metodą tarcia (Friction Stir Processing – FSP). Przyjęto, że zależność pomiędzy prędkością obrotową i momentem obrotowym jest funkcją eksponentyjalną. Natomiast dla wyznaczenia zależności pomiędzy prędkością przesuwu i siłą docisku użyto funkcji liniowej. Metodą sieci neuronowych ustalono zależność wartości parametrów technologicznych

i momentu obrotowego narzędzia. Analiza wyników badań wykazała, że zwiększenie prędkości obrotowej powoduje zmniejszenie momentu, natomiast wzrost prędkości przesuwu i siły docisku wzrost momentu obrotowego. W badaniach stosowano odlewniczy stop aluminium AlSi9Mg. Stosowany proces FSP spowodował zmniejszenie porowatości w modyfikowanej warstwie wierzchniej stopu oraz rozdrobnienie jego ziaren.

Słowa kluczowe: tarcowa modyfikacja, moment obrotowy, stopy aluminium

1. Introduction

Address: Marek S. WĘGŁOWSKI, PhD Eng., Institute of Welding, Testing of Materials Weldability and Welded Structures Department, Bl. Czesława 16-18 street, Gliwice 44-100, e-mail: marek.weglowski@is.gliwice.pl

Friction Stir Processing (FSP) is an efficient solid state modification process that have numerous potential applications in many industries including automotive, machine building, aerospace, as well as in the armaments industries. It combines frictional heating and stirring motion to soften and mix the surface layers in materials, in order to produce fully modified area. One of its main advantages lies in the possibility of modifying materials previously difficult to be processed, and obtaining new useful properties. A FSP tool consists of a shoulder of a larger diameter and a smaller probe - pin. The shoulder provides the primary source of heat by friction, prevents the material expulsion, and assists the material movement around the tool. The pin's primary function is to mix the material under the tool shoulder, which can be enhanced by threads. FSP is actually performed in three steps. First, the pin is plunged into the modified surface, until the shoulder gets in contact. As the tool rotates at a high velocity, the sheets are heated up by plastic deformation and friction. Second, the tool keeps rotating without any travelling motion, so the material heating due to friction increases. Finally, the tool moves along the modification designed line, heating the material further, moving it from the front of the tool, and depositing it behind its trailing edge, so producing the modified area. This process is shown in Fig. 1.

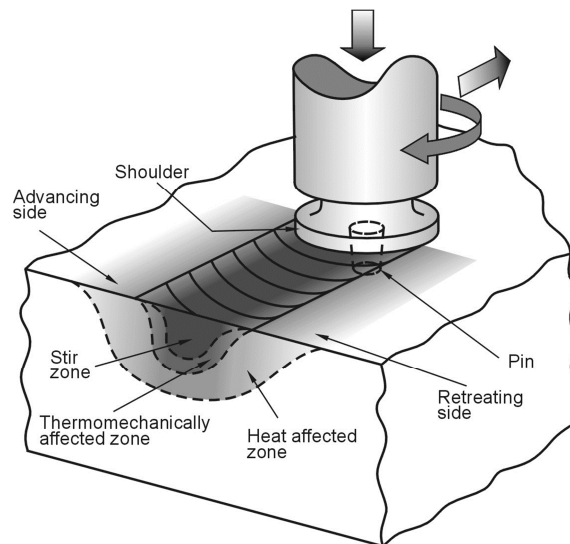


Fig. 1. Scheme of friction stir processing process

Determining a model for the torque is an important stage in estimating an overall heat input model for FSP. A heat input model would allow FSP parameters to be selected for desired properties of the modified surface. Various methods have been utilized to model the generation and transfer of heat during

friction stir process. These include experimental techniques [1-2] analytical methods [3, 4] as well as those based on finite element analysis [5, 6] and computational fluid dynamics [7].

The effects of rotational (ω) and travelling (v) speeds on torque and temperature have been widely reported in other papers [8]. Cui et al. [2] observed that the torque is more strongly influenced by the rotational speed rather than travelling speed. It was also suggested that torque, expressed as energy input per revolution, is determined by the material flow volume per the shoulder revolution. Arbogast [9] showed that the volume of flowing material increases when the rotational speed increases. This is the result of the processed material sticking to the shoulder due to its excessive heating caused by friction forces. Arora et al. [10] provided evidence that the computed torque decreases with the increase in the rotational speed. Such a behaviour was rationalized by the easier flow of the material at higher temperatures and strain rates. The computational results were consistent with the experimental results. The authors also noticed that the decrease in torque with decreasing travelling speed at constant rotational speed may be due to two contributing factors. From one side, for the constant tool rotation speed and decreasing travelling speed, the volume of material being deformed on each revolution decreases, hence the heat is generated in a smaller volume. This in turn may lead to slightly higher temperature and lower flow stress. From the other side, lower travelling speeds reduce the convective cooling, resulting from slower movement into the relatively cooler material in front of the tool. Peel et al. [11] pointed out that both, the torque and the extent of material mixing in the stir zone, display the much stronger dependence on the rotational speed than the travelling one.

The objective of this work is to determine the relationship between travelling and rotational speed of the FSP tool, down force and torque acting on the tool. One major difference between the present work and the previous ones, quoted in literature, is a wider range of rotational and travelling speeds applied in the experiments as well as more precise measurement of the torque acting on the tool. The experimental results are compared with the neural network model.

2. Methodology

Friction Stir Processing experiments were conducted on a conventional vertical milling machine specially adapted for experiments. The work stand was provided with the necessary instrumentation such as clamps for rigid fastening of the modified plates and a tool-cooling system employing compressed air. Additionally, the stand was equipped with LOWSTIR measurement head. The LOWSTIR system recorded: transverse force, down force and spindle torque. The FSP tool was made of HS6-5-2 high speed steel. The tool constitutes a shoulder 20 mm in diameter and a threaded pin 4,5 mm in length and 8 mm in

diameter. The tool tilt angle was kept constant at $1,5^\circ$. The rotational speed was varied from 112 to 1800 rpm while the travelling one was in the range of 112÷1120 mm/min. The lengths of the processed areas were approximately constant, about 180 mm. The material used in experiments was a commercial cast aluminium alloy AlMg9Si in the form of plates of dimensions 450×100×6 (length×width×thickness) mm. The alloy was not subjected to heat treatment before processing. The plates were firmly fixed to the machine table by suitable grips. The plate surfaces were not cleaned before processing. The roughness of the surface was as directly after milling.

The mean value of the spindle torque, travelling force and down force were measured by LOWSTIR and calculated from 100 points at the area of the fully stabilized FSP process. It should be emphasized that the signals recorded during FSP are characteristic for the specific tool geometry, parameters of the process, base material, measurement system (LOWSTIR) and experimental setup. The multiple regression model was generated using Statistica software.

The microstructure of the as-received and processed material was characterized by light microscopy (LM). Specimens were cut out perpendicularly to the direction of processing. The samples were mechanically grounded and then polished with a diamond paste. The final polishing was accomplished using Al_2O_3 suspension of about 0,25 μm . The observation was carried out without etching of the samples.

3. Results and discussion

The influence of the rotational and travelling speeds on the torque is shown in Figures 2a and 2b, respectively. It is evident from Figure 2a that the spindle torque strongly depends on the rotational speed of the FSP tool. This is because the rotational speed (the increase the linear speed of material flow) stimulates the temperature in the FSP area (modified material) [12] and thus the increase in the temperature reduces the local shear strength, resulting in the reduction of friction coefficient. However, the torque is not significantly affected by the change in the travelling speed. The predominant role of the rotation speed corresponds with the results presented by Cui et al. [2] and Arora et al. [10]. The mathematical correlation between rotational and travelling speed and torque are given in Tables 1 and 2, respectively. The relationship between rotational speed and torque was modelled by an exponential function. The dependence of the travelling speed and down force affecting the torque was successfully approximated by linear functions.

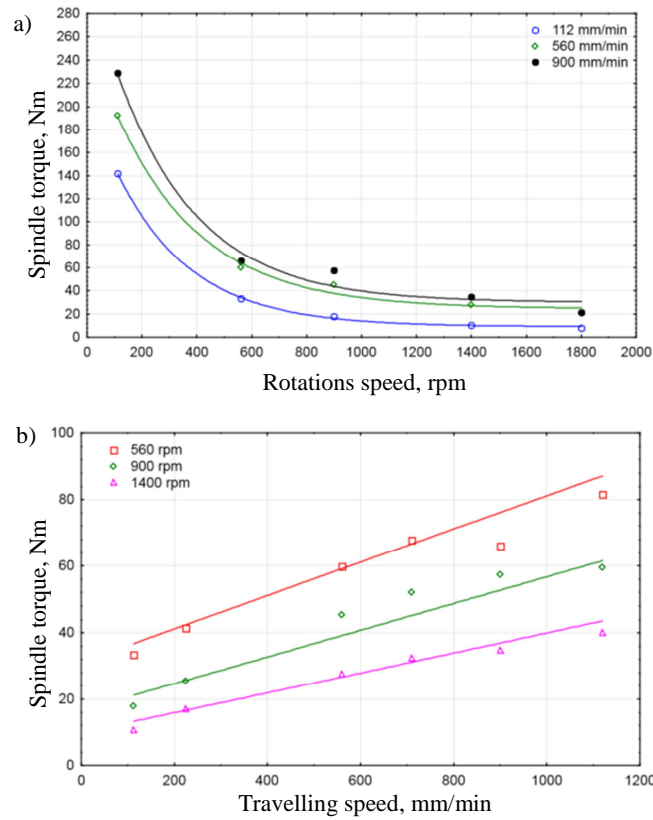


Fig. 2. Influence of (a) rotational speed and (b) travelling speed on torque

Table 1. The modelled relationship between rotational speed and torque acting on the tool

Travelling speed, mm/min	Modelled relationship
112	$M_{112} = 201,16 \cdot \exp\left(-\frac{\omega}{268,71}\right) + 9,18$
560	$M_{560} = 240,17 \cdot \exp\left(-\frac{\omega}{310,21}\right) + 24,57$
900	$M_{900} = 289,70 \cdot \exp\left(-\frac{\omega}{295,39}\right) + 30,03$

Table 2. The modelled relationship between travelling speed and torque acting on the tool

Rotational speed, rpm	Modelled relationship
560	$M_{560} = 31,15 + 0,05 \cdot v$
900	$M_{900} = 16,75 + 0,04 \cdot v$
1400	$M_{1400} = 9,94 + 0,03 \cdot v$

In the case of the FSP process the movement is composed of linear and rotational motion. Hence, the value of the pitch (travelling speed/rotational speed) is an important factor in determining the load of the tool. The impact of pitch (p) on the value of spindle torque at a constant rotational speed and travelling speed was investigated.

The influence of a pitch on the torque is presented in Figures 3a and 3b. The mathematical correlations between a pitch and torque at constant rotational and travelling speed are given in Tab. 3 and 4, respectively. The results indicate that an increase of the pitch increases the torque. This is due to the fact that the increase in the pitch is associated with an increase in travelling speed (at constant rotational speed) and for that as shown in Fig. 2b, the torque increases. In the case of the increase in the pitch at a constant travelling speed, the increase in the value is associated with a reduction of rotational speed, which results in (Fig. 2a) the torque increase.

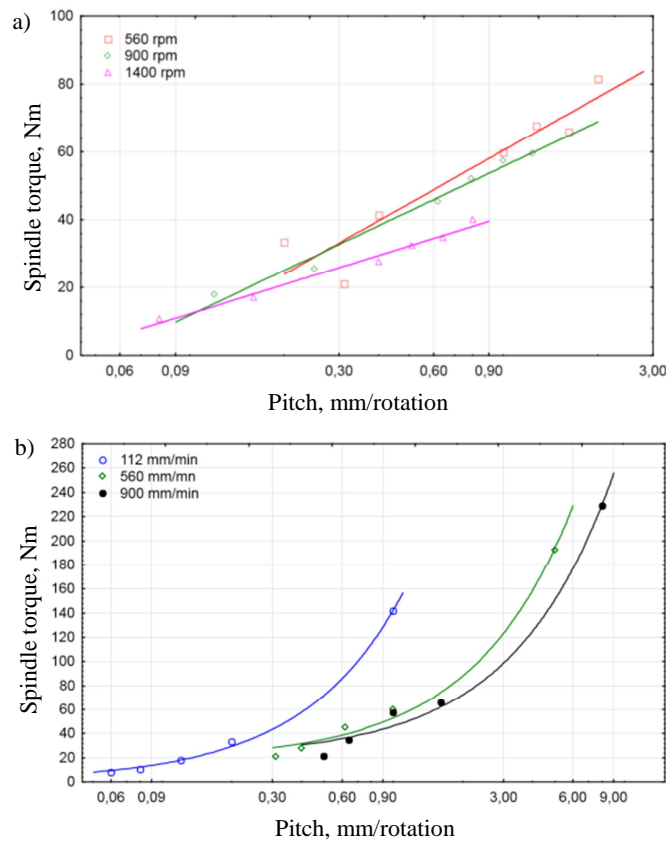


Fig. 3. The influence of pitch on the torque: a) at constant rotational speed, b) at constant travelling speed

Table 3. The modelled relationship between pitch and torque acting on the tool at constant rotational speed

Rotational speed, rpm	Modelled relationship
560	$M_{560} = 60,43 + 52,16 \cdot \log(p)$
900	$M_{900} = 55,68 + 43,90 \cdot \log(p)$
1400	$M_{1400} = 40,84 + 28,66 \cdot \log(p)$

Table 4. The modelled relationship between pitch and torque acting on the tool at constant travelling speed

Travelling speed, mm/min	Modelled relationship
112	$M_{112} = 1,15 + 141,24 \cdot p$
560	$M_{560} = 17,63 + 35,21 \cdot p$
900	$M_{900} = 20,12 + 26,17 \cdot p$

The influence of down force on the torque acting on a tool, presented in Fig. 4, shows that the increase of force causes the increase of torque, which is common phenomenon.

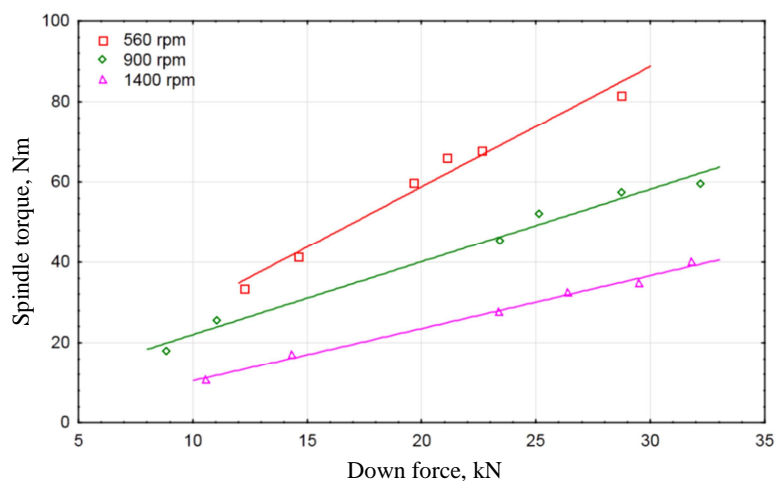


Fig. 4. Influence of down force on spindle torque at constant rotational speed

The value of spindle torque is influenced by rotational speed, travelling speed, down force, type and shape of the tool, and a kind of the modified material. To find the dependence combining the torque acting on the tool with the rotational speed in a wider range (112÷1800 rpm), the travelling speed in the

range of 112÷1120 mm/min and down force, artificial neural networks were applied. The neural net was built by means of an automatic net creator from the neural network software (Statistica). Rotational and travelling speeds and down force were introduced as input to the neural network (Tab. 5). The automatic creator tested successively 200 nets, while the quantity of the learning subset was 70%, validation subset – 15% and testing subset – 15%. As the result the three-layer perceptron net type 3:2-4:1 was chosen (Fig. 5).

Table 5. The modelled relationship between down force and torque

Rotational speed, rpm	Modelled relationship
560	$M_{560} = -1,19 + 3,0 \cdot F_d$
900	$M_{900} = 3,93 + 1,81 \cdot F_d$
1400	$M_{1400} = -2,65 + 1,31 \cdot F_d$

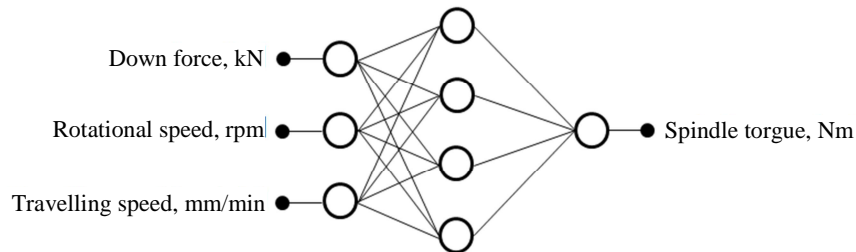


Fig. 5. Architecture of the optimal multilayer perceptron net, characterized by one hidden layer with 4 neurons, used to solve the regression problem

The results of calculations with the linear function defining the relationship between the actual and calculated values of torque for the learning subset are shown in Fig. 6. These charts give insight into how exactly the network output reflects the actual value of the output variable. The graphs line $y = x$ facilitates the observation. Of course, points do not lie exactly on the line $y = x$. The reason for this "non-compliance" is that the noisy data prevent the network from fitting them properly.

Figure 7a shows light microscopy micrograph of AlSi9Mg castings in the as-received condition. Coarse acicular Si particles were distributed along the primary aluminium dendrite boundaries. Furthermore, the material exhibited numerous pores. Figure 7b depicts microstructure of the processed AlSi9Mg alloy. FSP resulted in a significant refinement of large Si particles and subsequent uniform distribution in the aluminium matrix. Furthermore, porosity in the as-cast AlSi9Mg was nearly eliminated by FSP. Intensive plastic deformation and material flow at higher temperature induced by the stirring action of the tool and friction force are responsible for the grain refinement and

dynamic recrystallisation in the processed area. The FSP also removes casting pores and homogenizes the microstructure.

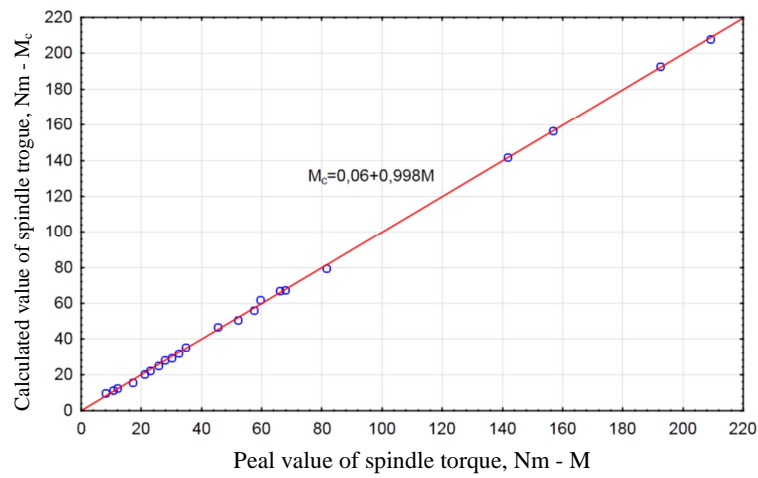


Fig. 6. Results of calculation of torque by the neural networks 3-4-1, learning subset

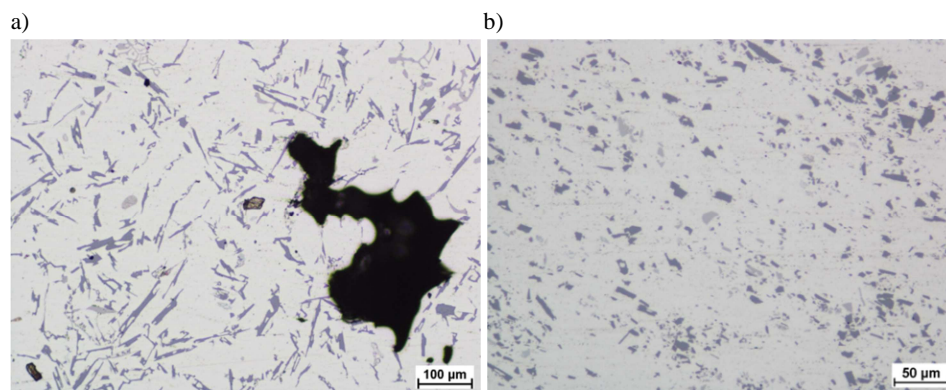


Fig. 7. The Microstructure of: a) as-cast AlSi9Mg alloy, b) FSP AlSi9Mg alloy at travelling speed of 560 mm/min and rotational speed 560 rpm

Summary

This study has examined the relationship between parameters of FSP process and torque acting on the tool during modified AlSi9Mg alloy. The results were as follows:

- the increase of the rotational speed decreases the torque acting on the tool,
- the increase of the travelling speed does not influence the spindle torque acting on the tool substantially – only a slight increase was observed,
- the increase of the pitch at constant travelling speed increases the torque,
- the increase of the pitch at constant rotational speed increases the torque,
- the application of the neural network will make possible to determine the relationship between rotational and travelling speeds, down force and spindle torque,
- it was found that best regression results for the analysed case can be received by using the three-layer perceptron network type 3:2-4:1,
- the friction modified processing applied to the alloy surface causes the refinement of microstructure in the near-surface layer and reduces porosity.

Acknowledges

This publication is a result of research performed with the funding from the Ministry of Science and Higher Education in Poland within the frame of statutory activity of Institute of Welding – Gliwice.

References

- [1] M. ASSIDI, L. FOURMENT, S. GUERDOUX, T. NELSON: Friction model for friction stir welding process simulation: Calibrations from welding experiments. *Int. Journal Machine Tool Manufacture*, **50**(2010), 143-155.
- [2] S. CUI, Z.W. CHEN, J.D. ROBSON: Interrelationships among speeds, torque and flow volumes during friction stir welding/processing. Proc. 8th International Friction Stir Welding Symposium, Timmendorfer Strand, 2010.
- [3] H. SCHMIDT, J. HATTEL, J. WERT: An analytical model for the heat generation in friction stir welding. *Modelling Simulation Materials Science Engineering*, **12**(2004), 143-157.
- [4] P. KALYA, K. KRISHNAMURTHY, R.S. MISHRA, J.A. BAUMANN: Specific energy and temperature mechanistic models for friction stir processing of AL-F357. Proc. of Friction Stir Welding and Processing IV, 113-125, Florida 2007.
- [5] C. HAMILTON, S. DYMEK, A. SOMMERS: A thermal model of friction stir welding in aluminum alloys. *Int. Journal Machine Tool Manufacture*, **48**(2008), 1120-1130.
- [6] H.W. ZHANG, Z. ZHANG, J.T. CHEN: The finite element simulation of the friction stir welding process. *Materials Science Engineering, A*, **403**(2005), 340-348.
- [7] T. LONG, A.P. REYNOLDS: Parametric studies of friction stir welding by commercial fluid dynamics simulation. *Science Technology of Welding and Joining*, **11**(2006), 200-208.
- [8] J.W. PEW, T.W. NELSON, C.D. SORENSEN: Torque based weld power model for friction stir welding. *Science Technology of Welding and Joining*, **12**(2007), 341-347.

- [9] W.J. ARBEGAST: A flow-partitioned deformation zone model for detected formation during friction stir welding. *Scripta Materialia*, **58**(2008), 372-376.
- [10] A. ARORA, R. NANDAN, A.P. REYNOLDS, T. DEBROY: Torque, power requirement and stir zone geometry in friction stir welding through modelling and experiments. *Scripta Materialia*, **60**(2009), 13-16.
- [11] M.J. PEEL, A. STEUWER, P.J. WITHERS, T. DICKERSON, Q. SHI, H. SHERCLIFF: Dissimilar friction stir welds in AA5083-AA6082. Part I: Process parameter effects on thermal history and weld properties. *Metallurgical and Materials Transactions A*, **37**(2006), 2183-2193.
- [12] M.S. WĘGŁOWSKI, A. PIETRAS, S. DYMEK, C. HAMILOTN: Characterization of friction stir processing applied for modification of surface microstructure in a cast aluminium alloy. Proc. 14th Inter. Conf. Metalforming, 2012, 587-590.

Received in January 2013